npj Urban Sustainability

https://doi.org/10.1038/s42949-026-00351-y

Article in Press

COVID-19 and urban exodus: diverging population redistribution patterns across countries from 2020 to 2022

Received: 27 May 2025

Accepted: 29 January 2026

Cite this article as: Duan, Q., Lai, S., Sorichetta, A. *et al.* COVID-19 and urban exodus: diverging population redistribution patterns across countries from 2020 to 2022. *npj Urban Sustain* (2026). https://doi.org/10.1038/s42949-026-00351-y

Qianwen Duan, Shengjie Lai, Alessandro Sorichetta, Andrew J. Tatem, Jessica Steele & Felix Eigenbrod

COVID-19 and urban exodus: diverging population redistribution patterns across countries from 2020 to 2022

Qianwen Duan [a] *, Shengjie Lai [b], Alessandro Sorichetta [c], Andrew J. Tatem [b], Jessica Steele [b], Felix Eigenbrod [a]

[a] School of Geography and Environmental Science, University of Southampton, Southampton SO17 1BJ, United Kingdom

[b] WorldPop, School of Geography and Environmental Science, University of Southampton, Southampton SO17 1BJ, United Kingdom

[c] Dipartimento di Scienze della Terra "Ardito Desio", Università degli Studi di Milano, Via Mangiagalli 34, 20133 Milan, Italy

* Corresponding author: Qianwen Duan Q.Duan@soton.ac.uk

Abstract

While widespread urbanisation continues, emerging trends of population redistribution away from highly urbanised areas have been observed in some countries, with important implications for infrastructure planning, resource allocation, and environmental risk assessment. However, few studies have examined this trend in a timely and spatially comprehensive manner across diverse national contexts, particularly in response to the turbulence in migration patterns caused by the COVID-19 pandemic. Here, we analyse spatial Facebook population data from 2020 to 2022 across 35 countries to characterise two forms of population redistribution: shifts between urban and rural areas, and changes along the urban density gradient. During the early response phase of the pandemic, broader country-level trends of urban-to-rural redistribution and intra-urban deconcentration were evident. However, 20% and 4.8% of these trends, respectively, were temporary and reversed during the later phase of the pandemic. The extent and direction of these patterns varied across countries and were negatively associated with the Human Development Index, suggesting that developed nations experienced greater urban depopulation and spatial deconcentration. Our findings reveal a potential misalignment between population redistribution and existing physical urban densities in certain countries, as densely built-up areas are experiencing outflows, highlighting the need for adaptive urban planning strategies to address evolving population dynamics and related sustainability challenges.

Introduction

Our world has experienced rapid urbanisation over the past few decades. From 1960 to 2020, the urban population increased from 1.0 to 4.4 billion, with over 50% of inhabitants living in urban areas [1]. In general, this increasing trend is widely expected to continue [2]. However, a contrasting phenomenon of urban depopulation has occurred in some countries, particularly in the Global North, where populations are relocating to less urbanised areas [3,4]. Although this shift may remain modest and in its early stages compared to the dominant trend of urban growth[5], it may signal long-term changes. It is predicted that half of US cities will experience population loss by 2100 [6]. More recently, the COVID-19 pandemic and interventions triggered an unprecedented global shock to migration patterns [7,8]. Lockdowns, fear of COVID-19 spread, and shifts in lifestyle such as the rise of remote work led many people to reconsider

their living environments, sparking a growing interest in less urbanised areas during the pandemic [9,10]. These shifts raise important questions about the future of urbanisation and whether the traditional assumption of ever-growing populations in cities needs to be reconsidered.

Understanding changes in population distributions across varying urbanised areas is important for various fields, from infrastructure planning [6,11] to resource allocation [12] and environmental risk assessment [13–15]. Most past planning assumed that urban populations would continually grow [7]. Our research aims to explore whether this trend is shifting, particularly in response to the shock of COVID-19, and highlights the need to adapt future planning accordingly. For example, highly urbanised areas experiencing population declines may no longer require extensive construction and investment due to existing underutilised infrastructure and should instead focus on maintaining them [6,16]. Conversely, rural and peri-urban areas facing an influx of new residents may require enhanced public services and transportation networks. Meanwhile, the reshaping of derelict land in depopulated built areas [6], alongside the revitalisation of landscapes in areas with increased population [13], presents new environmental opportunities and challenges.

However, traditional data sources often fall short in capturing timely and spatially detailed population changes. Spatial population maps, which usually allocate populations based on layers including satellite imagery-derived settlement extents and land cover types, do not accurately provide real-time population shifts and migration patterns within those extents [17]. Recently, the growing availability of mobile phone location data from the Global Positioning System (GPS) and online social media and smartphone applications of digital platforms, such as Google [18], Apple [19] and Meta (Facebook) [20–22], provides new opportunities to better understand near-real-time population distributions across space and time, although user representation biases exist. For example, Facebook data derived from aggregated user location history have been used to assess population exposure to climate risks and monitor density changes during disasters and emergencies [23–25]. During the COVID-19 pandemic in particular, these data were invaluable for tracking mobility patterns [22,26] and urban–rural shifts [20,27–29]. Yet, most existing studies using such data to examine urban–rural shifts have focused on individual countries or regions [27,30,31] due to limited data access, leaving little understanding of the common characteristics underlying patterns of population redistribution in different socio-economic settings. Additionally, while the pandemic might have influenced shifts in population distribution, it remains unclear whether these changes were merely temporary.

In this study, we seek to answer two questions: 1) how has population distribution across various urbanised areas changed during COVID-19 across different countries; 2) what socioeconomic characteristics were associated with the heterogeneity in country-level population redistribution patterns. Using spatially referenced Facebook population data from Meta [21] during night-time and following a recently developed pre-processing approach [20] (see Methods), we analysed trends in population distribution from 2020 to 2022 across varying urbanised areas in 35 countries (23 high-income and 12 middle-income). Physical urban density (% of built-up areas; Supplementary Fig. 3) was used to characterise degrees of urbanisation, and is considered to be closely linked to infrastructure distribution [32,33]. Our findings provide valuable insights into both cross-national and fine-grained patterns of population redistribution in response to COVID-19, and also contribute to a broader understanding of urban–rural continuum dynamics, highlighting the importance of adaptive urban planning, policy, and resource management in a post-pandemic world.

Results

For each country, we analysed population redistribution patterns by examining changes in urban-rural distribution and along the urban density gradient. To quantify these patterns at the country level, we calculated two indicators separately: (1) the change in urban population proportions, and (2) the Spearman correlation coefficient for each country, computed between population changes and urban density values across individual Facebook tiles (Fig. 1). These indicators were then examined in relation to socioeconomic characteristics to identify potential underlying drivers of country-level differences.

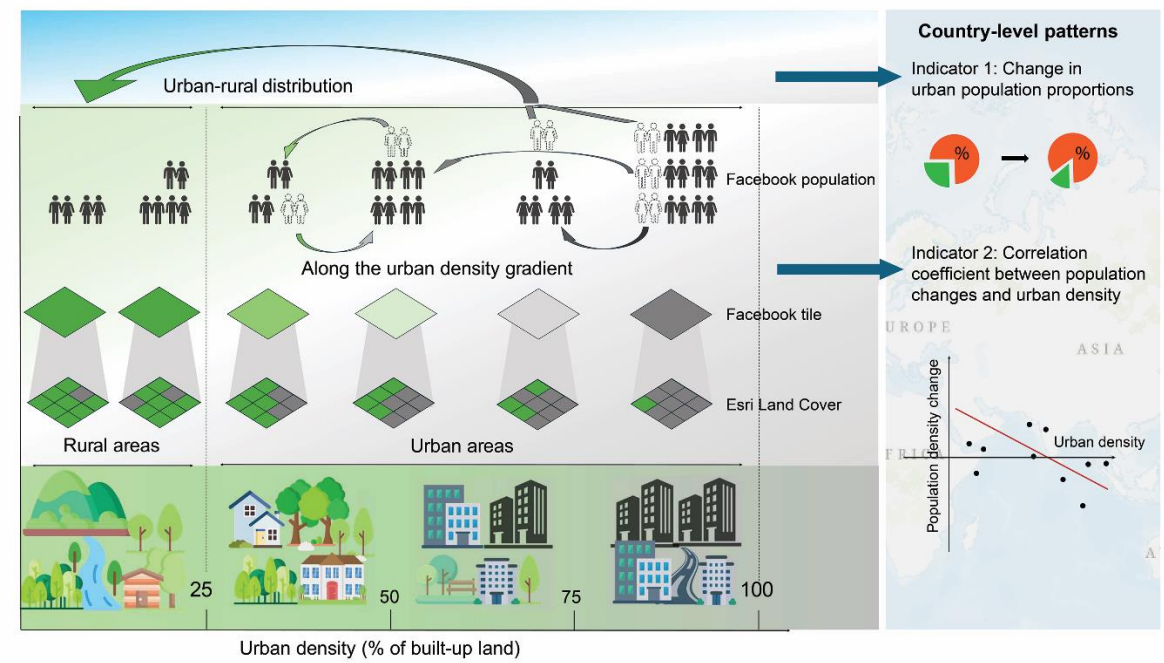

Fig. 1 The analytical framework for quantifying patterns of population redistribution. Colour transitions from green to grey represent a gradient from very low to very high urban density. Facebook data (tile level) were overlaid with the "built-up area" class from the Esri 2020 Land Cover dataset to characterise population changes across the urban density gradient within each country. Two country-level indicators (Indicators 1 and 2) were calculated based on tile-level data for each country (see Methods), to quantify shifts between urban and rural areas and changes along the urban density gradient, respectively. This figure was created using resources from Flaticon.com, with specific author attributions provided in the Acknowledgments.

Changes in urban-rural population distribution

Given the varying impact of COVID-19 on population dynamics across countries during the study period (March/April/May 2020 to May 2022; see Supplementary Table 5), we applied a data-driven structural breakpoint analysis to weekly urban population proportion data (See Methods; Supplementary Fig. 4). This automatically identified a single significant breakpoint for most countries, allowing us to define two phases: Phase 1 (early response phase) and Phase 2 (later response phase). The approach reflects actual

changes in population distribution in responses to the pandemic and associated restrictions, informed by previous work indicating that major shifts often correspond with critical pandemic response stages [20], and accounts for the fact that even identical restrictions may have had different effect and levels of public compliance across pandemic waves and countries [34,35].

Urban areas were defined as regions with urban density exceeding 25%, while areas below this threshold were classified as rural, based on a commonly used definition from the perspective of physical urban land [37,38]. Sensitivity tests with alternative cutoffs (20%, 30%, 40% and 50%) were used to estimate breakpoints and the direction and extent of changes in urban population proportions. These tests showed no statistically significant differences compared to the 25% threshold ($P > 0.5$; see Supplementary Fig. 5), confirming the robustness of our classification.

Our findings revealed notable cross-country variations in urban population changes over time (Indicator 1; Figs 1 and 2A). While over 70% of countries maintained consistent trend directions across both phases, differences in magnitude were evident. Specifically, 13 out of 35 countries (37.1%) experienced declining trends in urban population proportions in both phases, with six (New Zealand, South Korea, Argentina, Iceland, Chile and Bhutan) showing greater declines in Phase 2. Conversely, 12 countries experienced increasing trends throughout both phases, with four (Cambodia, Morocco, Spain, Japan) showing larger increases in the later phase. Additionally, 10 countries exhibited contrasting trend directions between the two phases, indicating that the choice of living in urban or rural areas for many of their population was impacted by the COVID-19 pandemic. Overall, more countries demonstrated a decreasing trend in Phase 1 (Fig. 2B).

When comparing urban population proportion changes between countries grouped by Human Development Index (HDI), clear disparities emerged. Countries with very high HDI (>=0.8) showed a negative mean change, with a smaller decrease in Phase 2 (-0.199%/year) compared to Phase 1 (-0.423%/year). In contrast, countries in middle & high HDI group (<0.8) displayed positive mean changes, increasing slightly from Phase 1 (0.702%/year) to Phase 2 (0.790%/year) (Fig. 2C).

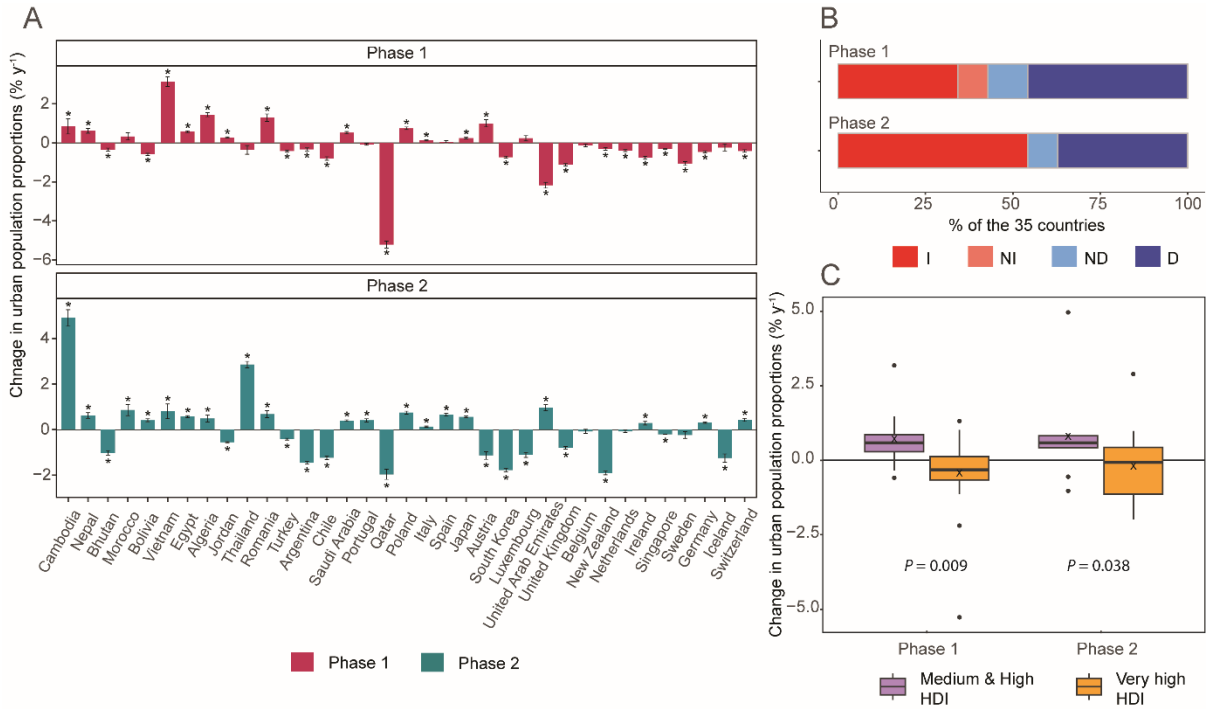

Fig. 2 Contrasting patterns of change in urban population proportions across countries (Indicator 1). **(A)** Changes in urban population proportions, estimated using robust linear regression on weekly proportion data. Error bars represent standard errors of the regression estimates, and asterisks (*) denote statistical significance level ($P < 0.05$). Significance was assessed using the two-sided robust F-test with the "sfsmisc" package in R [39]. **(B)** Share of countries by change category: I for significant increase, NI for non-significant increase, ND for non-significant decrease, and D for significant decrease ($P < 0.05$). **(C)** Box plots of changes between countries with middle & high (< 0.8; n = 10) and very high (>= 0.8; n = 25) Human Development Index (HDI) levels. Boxes show the 25th to 75th percentiles, with the median as a central line and the mean marked by "X." Whiskers extend 1.5 times the interquartile range. Significant differences between groups were tested using the two-sided Wilcox test.

Change in population density along the urban density gradient

To further examine the nuances of population shifts, we assessed changes in population density at the Facebook tile level within each country (see Methods). Our analysis revealed distinct spatial patterns for each country (Fig. 3, see additional country plots in Supplementary Figs. 6 and 7). Although urban core trends varied between countries, peripheral areas often exhibited shifted in the opposite direction relative to their cores. For instance, during Phase 2, Cambodia showed population growth in urban cores and declines in surrounding areas, whereas the UK and South Korea experienced population losses in urban cores and growth in the periphery.

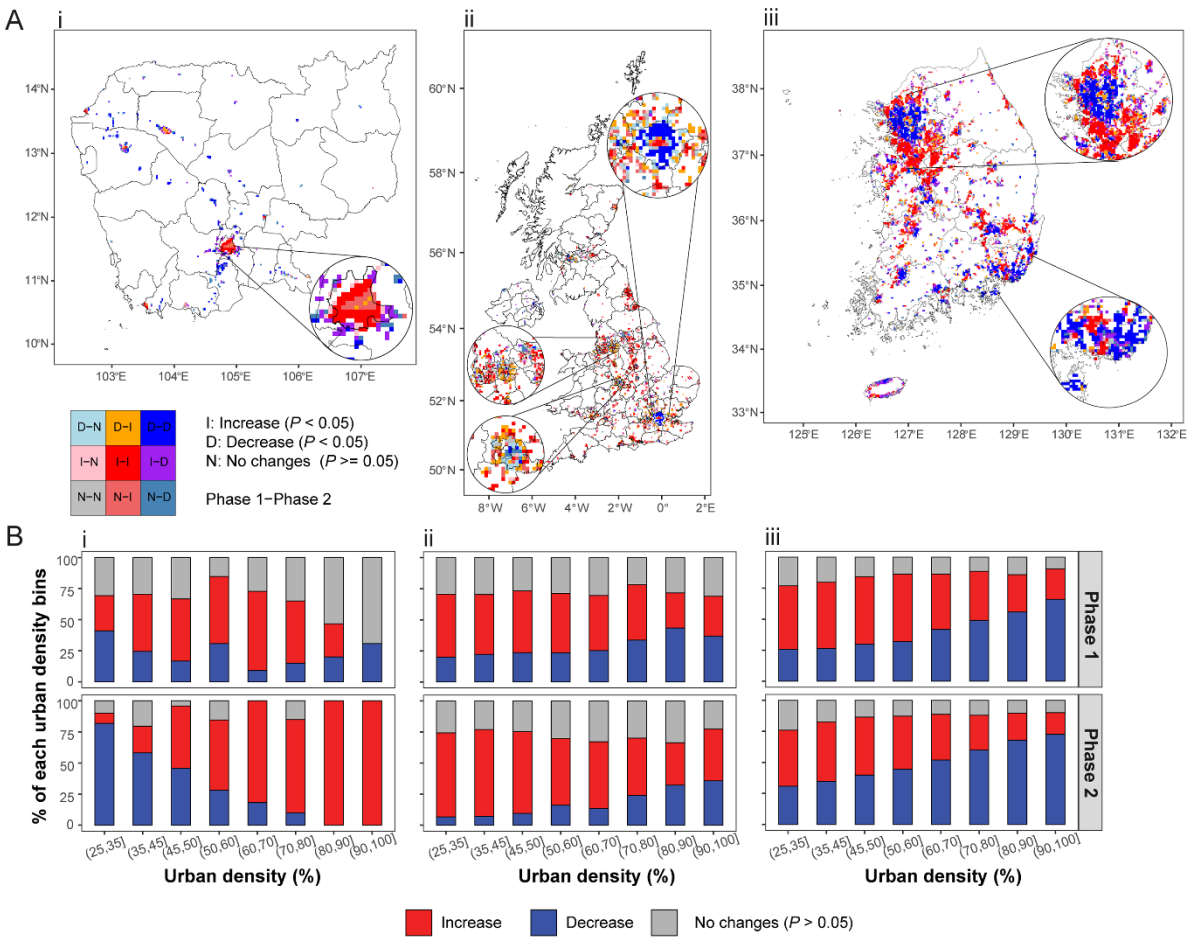

Fig. 3 Spatial patterns of population density changes across urban density gradient within urban areas. **(A)** Maps of population density change categories in urban Facebook tiles during two phases for two example countries: (i) Cambodia, (ii) the United Kingdom and (iii) South Korea. See additional country maps in Supplementary Fig. 6. Phase segmentation for each country has shown in Supplementary Fig. 4. **(B)** Share of population density change categories along urban density bins. Bins were set at 5% increments for the lower 50% urban density and 10% increments beyond 50%, accounting for the uneven distribution of urban density, as a greater number of tiles have lower densities. See additional country plots in Supplementary Fig. 7. Country and administrative boundaries were sourced from the Global Administrative Areas (GADM) spatial database (version 4.1).

To quantitatively summarise each country's trend of deconcentration or concentration along urban density gradient, we calculated Spearman correlations by comparing population changes with urban density values across individual Facebook tiles (Indicator 2; Figs. 1 and 4A). A modified t-test to was applied to evaluate the statistical significance of the correlations [40], accounting for significant spatial autocorrelation detected in all 35 countries (See Supplementary Table 6). A greater number of countries showed significantly negative correlations in Phase 2 (Fig. 4B). However, no significant differences in correlation coefficients were observed between the very high HDI and middle & high HDI groups in either phase ($P > 0.05$; Fig. 4C). While the mean correlation coefficient was negative in the very high HDI

countries, suggesting greater population dispersion, it remained positive in the medium & high HDI groups, reflecting continued urban centre concentration in those regions.

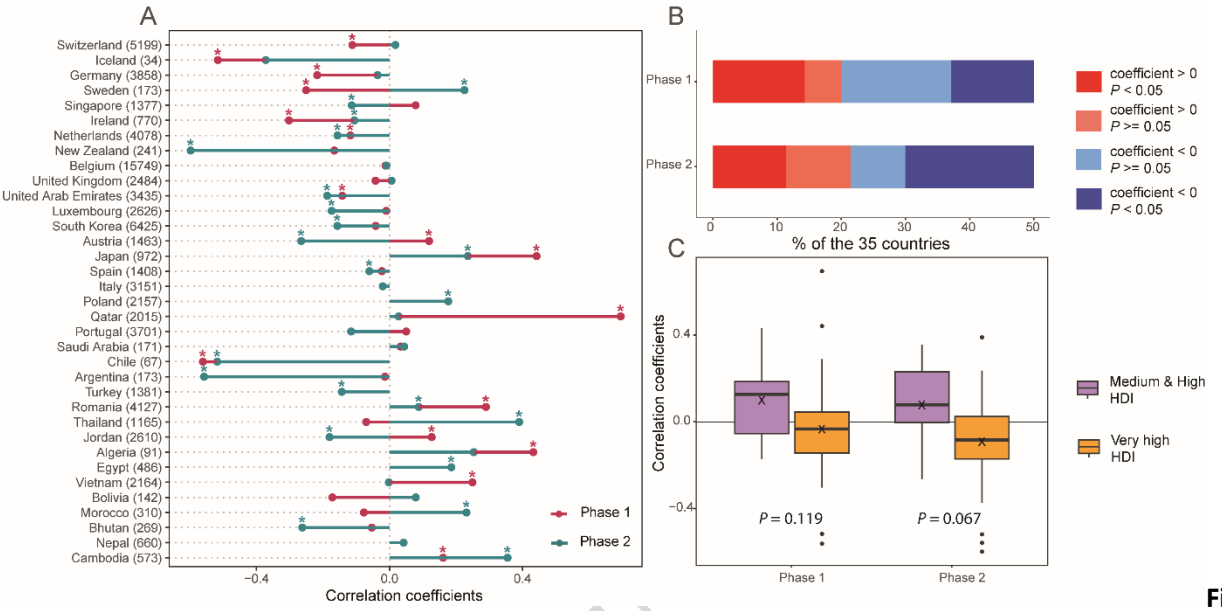

Fig. 4 Correlation between population density changes and urban density (Indicator 2). (A) Spearman correlation coefficients; statistical significances were assessed using the modified t-test (*$P < 0.05$). The numbers in brackets indicate the number of urban area tiles used in the calculation. **(B)** Share of countries by correlation category. **(C)** Box plots of correlation coefficients for countries with middle & high (< 0.8; n = 10) and very high (>= 0.8; n = 25) HDI levels. Boxes show the 25th to 75th percentiles, with the median as a central line and the mean marked by "X." Whiskers extend 1.5 times the interquartile range. Significant differences between groups were tested using the two-sided Wilcox test.

Country-level population redistribution patterns and associated socioeconomic characteristics

By combining the two indicators of changes in urban population proportions and correlation coefficients between population density change and urban density, we identified distinct country-level population redistribution patterns (Fig. 5). For example, in Phase 2, Spain (ESP in Quadrant IV) showed an increase in urban population proportion but a negative correlation between population changes and the urban density. This indicates that population shifts in Spain were not strictly an urban-rural phenomenon but rather complex dynamics – a movement from both highly urbanised and rural areas into moderately dense areas. While these two indicators were uncorrelated in Phase 1 (regression slope = 0.01; 95% credible interval (CrI): -0.06 to 0.08), a significant positive correlation emerged in Phase 2 (regression slope = 0.13; 95% CrI: 0.08 to 0.17). This suggests that, in Phase 2, countries experiencing higher increases in urban population proportion also tended to have increased population concentrations in very high-density urban areas.

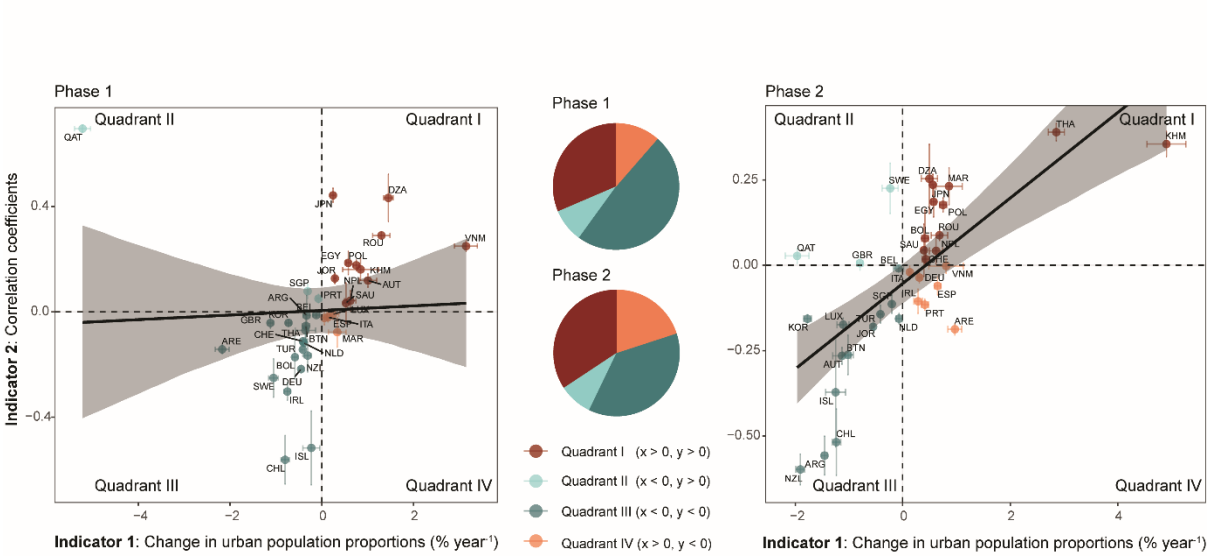

Fig. 5 Two-indicator summary of country-level population redistribution patterns. The x-axis represents the annual changes in urban population proportions (Indicator 1), while the y-axis shows the Spearman correlation coefficients between population density change and urban density (Indicator 2). The relationship between these two dimensions of urban population changes across 35 countries was fitted using a Bayesian linear model (black fitted line with a 95% credible interval). Pie charts in the centre display the proportion of countries in each quadrant for phase 1 (top) and phase 2 (bottom). Each country is marked using Country Codes Alpha-3 with the "countrycode" package in R [41].

The role of socioeconomic characteristics in shaping these redistribution patterns was further explored through Bayesian multivariate linear modelling (see Methods). Country-level heterogeneity in population redistribution patterns was negatively associated with HDI across both indicators and phases, except for correlation coefficients (Indicator 2) in Phase 1. Countries with higher HDI exhibited greater declines in urban population proportions (Phase 1: mean -0.48, 95% CrI -0.88 to -0.09; Phase 2: -0.68, 95% CrI -1.11 to -0.28) and more negative correlation coefficients (Phase 1: mean -0.05, 95% CrI -0.13 to 0.03; Phase 2: -0.15, 95% CrI -0.15 to -0.01) (Fig. 6). We also found statistical evidence of a negative effect of industrialisation on urban population proportions (Indicator 1: -0.45, 95% CrI -0.85 to -0.05) and a contrasting positive effect on correlation coefficients (Indicator 2: 0.08, 95% CrI 0.00 to 0.16) in Phase 1.

When compared these effects with results from competing models (Supplementary Fig. 8), we found similar patterns, although in some cases HDI showed strong evidence of negative association with correlation coefficients in Phase 1. In contrast, no credible associations were found between redistribution patterns and unemployment, income equality or the COVID-19 stringency index at the country level, indicating that other structural factors might play a more dominant role in shaping migration trends. A supplementary analysis of predictors excluded due to high correlation with HDI (Supplementary Fig. 9) found strong statistical support for a negative effect of government effectiveness and a positive effect of share of agriculture, forestry and fishing on changes in urban population proportions (Supplementary Fig. 10), while individualism showed no credible evidence of a negative effect.

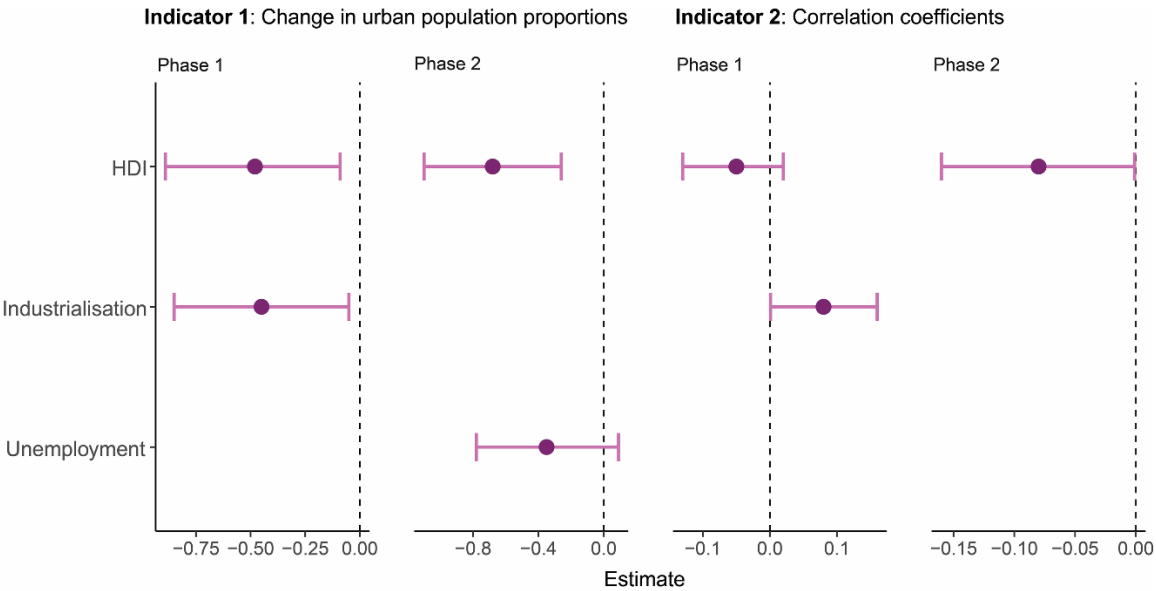

Fig. 6 Effects of socioeconomic characteristics on country-level population redistribution patterns. Indicator 1 is the change in urban population proportions (Phase 1: N = 35, R^2 = 0.25; Phase 2: N = 35, R^2 = 0.27). Indicator 2 is the Spearman correlation coefficients between population change and the urban density gradient (Phase 1: N = 35, R^2 = 0.19; Phase 2: N = 35, R^2 = 0.13). The mean posterior estimates of model parameters, with whiskers representing the 95% credible intervals for two indicators and phases were derived from Bayesian linear models. See Supplementary Table 9 for detailed posterior summaries for each variable.

Discussion

Our findings reveal broad yet heterogenous cross-country patterns of urban population redistributions in response to COVID-19, aligning with earlier reports of an "urban exodus" during the pandemic [27,42,43]. In the early stages of the pandemic, many countries experienced shifts toward rural or lower-density urban areas, as restrictions, health concerns, and lifestyle changes disrupted conventional patterns of urban living. Highly developed countries exhibited stronger trends toward urban depopulation and spatial deconcentration, while middle- and high-HDI countries largely continued along trajectories of urban population growth. However, some of these urban-rural shifts appear to have been temporary. In the later phase of the pandemic, a partial reversal of earlier trends was observed in several countries. Notably, countries that experienced larger increases in the proportion of urban populations also tended to show greater growth in highly urbanised areas, consistent with the view that rapid urbanisation is driven by the availability of more and better-paying jobs concentrated in urban cores [44]. In contrast, no such relationship was observed in the early phase, when migration patterns were more heavily impacted by the pandemic and its associated disruptions.

A notable result of this study is that the two indicators we used (urban population proportions and correlations between population change and urban density) are associated with similar country-level socioeconomic characteristics, though not always in the same way across the two phases. The

heterogeneity in population redistribution patterns across countries is negatively associated with HDI, aligning with previous observations in the Global North [4,45], which is typically features high living conditions and advanced education. This suggests that in more developed contexts, where health, education, and income are relatively high, even less urbanised areas can offer a high quality of life. Improvements in overall development provide better access to essential services and more natural environments [3] outside urban cores, reducing the need to live in densely urbanised areas [46]. This relationship is also consistent with findings from the IMAGE database, which show strong migration from low- to high-density areas in low-HDI countries, while very high-HDI countries tend to exhibit flatter or reversed trends [47]. The negative effect of industrialisation on urban population proportions in phase 1 may reflect disruptions to industrial sectors during the early pandemic, which prompted people to return to rural areas amid economic uncertainty and in search of family support. Similar patterns have been observed during past crises, where individuals moved away from cities as a survival strategy [48,49]. However, in phase 2, this effect turned positive, although not statistically credible, likely reflecting the diminished impact of the pandemic. A similar general positive effect of the industrialisation [51] on the correlations between population change and urban density further indicates that the pull of urban cores within metropolitan areas persisted even during the pandemic, aligning with the well-recognised notion that industrialisation enhances the attractiveness of cities and promotes urbanisation [50]. In addition, countries with higher government effectiveness or a lower share of agriculture, forestry and fishing showed credible decreases in urban population proportions. This suggests that high-quality public services and policy implementation improve rural liveability and appeal to potential migrants [52], while rural populations in agrarian economies remained attracted to urban areas, consistent with the rapid urban population growth observed in low-urbanisation countries that still rely on rural-based agricultural economies [53,54]. While we acknowledge that our analysis cannot capture all contributing factors, given the complexity of population redistribution and the constraints of global data availability, these findings nonetheless offer important implications for future planning.

Although it remains uncertain whether these trends will persist in the long term, the observed redistributions may signal future trajectories and highlight the importance of adapting future planning strategies tailored to countries' development levels. In very high-HDI countries, where the consistent depopulation in urban cores is accompanied by shifts to suburban or rural areas, short-term priorities include upgrading infrastructure in low-density areas to accommodate emerging demands [6], such as expanding broadband access to support remote work and improving transport connectivity. Long-term challenges include managing growth in recipient rural areas to prevent uncontrolled sprawl. At the same time, strategic planning is necessary for those remaining in cities, where rising inequality and poverty are growing concerns [6,16]. This includes maintaining and repurposing underutilised infrastructure in depopulating high-density areas, such as water and electricity systems [6,16], protecting low-income households from potentially rising service costs, and converting vacant land into green spaces to preserve urban liveability [55]. In contrast, middle- and high-HDI countries experiencing continued urbanisation should prioritise managing urban growth while preventing rural decline. This includes developing industries that support remote work to alleviate urban pressure and investing in rural infrastructure to enhance its attractiveness. However, as these countries continue to develop, long-term planning should also anticipate potential shifts from high- to low-density areas. Additionally, in agriculturally dominant economies, the observed rural-to-urban migration raises concerns about a potential long-term risk to food security, highlighting the need for governments to invest in rural development and agricultural technology to sustain a stable farming workforce.

Shifting patterns of population distribution bring both possibilities and challenges for environmental sustainability [13]. While there are concerns about extensive development and occupation of local natural habitats by incoming residents [56], evidence suggests that the environmental impact of this trend is complex and may not directly alter land use [13]. Migrants drawn to rural areas by the pursuit of better natural amenities often aim to protect and restore the landscapes, preserving the unique rural appeal that attracted them [13,57]. Meanwhile, the need to reshape idle infrastructure in depopulated cities poses challenges for urban sustainability and environmental equality for those remaining in high-density areas. Additionally, the shift from high- to low-density living raises concerns about increased energy consumption and its impact on environmental sustainability [6]. The exact environmental consequences of these changes require further exploration.

This analysis could also benefit resource allocation during future crises. Our finding that highly industrialised countries were most prone to a temporary urban exodus provides an important insight for preparedness [48]. Governments should anticipate that during a similar crisis, rural or low-density areas may experience temporary population increases. Crisis response strategies should therefore include increased allocation of medical supplies and essential goods to these regions [58], along with strengthened support for local services to manage the additional strain caused by a temporary influx of people.

However, these findings were identified from a limited sample of 35 countries, primarily from Europe, Aisa, and South America. Several major countries such as the United States, China, and India, as well as low-income countries were not included due to data unavailability or low Facebook penetration. While these exclusions were necessary to ensure data quality and reliability, they inevitably constrain the global generalisability of our findings. Therefore, our results should be interpreted with caution, as they reflect trends and patterns across countries with relatively high mobile and Facebook usage, and it remains unclear if these patterns extend more broadly. Nevertheless, this cross-national analysis provides valuable insights into broader dynamics across diverse contexts. Future research should explore complementary data sources to fill gaps in underrepresented regions.

A key methodological decision in this study was to define COVID-19 response phases using a data-driven approach based on population dynamics rather than relying on official policy timelines. This choice was based on extensive evidence of behavioural fatigue [35,59], where public adherence to interventions declines over time, causing a misalignment between government policies and actual population behaviour. For example, in the United States, early restrictions had a greater effect on social distancing than later interventions [60], and similar patterns have been observed in mobility behaviours across different COVID-19 waves [35,61]. Despite this, we found that the COVID-19 stringency index [36] generally declined or stabilised at a lower level following the identified breakpoint (Supplementary Fig. 11), and that differences between phases were statistically significant ($P < 0.05$) in most countries, except for Cambodia and those without identified breakpoints (Supplementary Fig. 12). We acknowledge that our period segmentation based on the dominant breakpoint may not fully capture temporal pattern in certain country (Supplementary Fig. 13). However, the consistent framework was essential for our primary objective of comparing population redistribution across countries.

Another major limitation of this study is that the Facebook population data include only users who have enabled location services, which may not accurately represent the overall population dynamics. Indeed, data for each country may be influenced by the penetration of smart mobile devices, Facebook app usage, and the use of location services [21,22]. To mitigate bias, we selected countries where Facebook app

coverage exceeded 40% [62]. However, since location services must be enabled on their devices, representativeness may be lower. Due to privacy protection constraints, no further user profiling information was available. Nevertheless, these data can reasonably represent population change trends [30] and capture migration patterns, as Facebook users typically belong to groups with high mobility [27], especially since our study focuses on those who lived in high-density areas before moving away. To assess the spatial reliability of our dataset, we correlated the tile-level Facebook baseline count (mean over 90 days before the study period) with the widely used gridded population dataset GHS-POP 2020 [63], both representing populations before the COVID-19 pandemic. Across countries, correlations ranged from 0.61 (Bhutan) to 0.98 (Portugal and Argentina), with over 94% exceeding 0.80 (Supplementary Fig. 2). Furthermore, using the United Kingdom as an example, we validated our estimates against 2021 Census data. Wider comparisons are challenging due to a lack of relevant census data during the pandemic; indeed, this lack of available data across countries is the reason we use Facebook data in this study. We found a high correlation of 0.97 between Facebook- and census-derived [64] population densities (Supplementary Fig. 15), as well as a moderate positive correlation of 0.55 between Facebook population trend and net migration from census origin-destination migration flows [65] (Supplementary Fig. 16) for England and Wales. The underestimation of change in the Facebook population is expected, as not all individuals use the platform or consent to data sharing. Together, these results validate the ability of our analysis to capture both real-world spatial patterns and migration trends. Other research using Facebook data in specific countries further support its reliability. Studies from the United Kingdom [26] and the United Sates [66] found Facebook data correlated well with census data, with no strong biases in age, ethnicity or race distributions. In Italy, although individuals aged 54 and above were underrepresented, this did not introduce spatial bias, as the territorial demographic distribution of age groups was relatively homogeneous [29]. In the Philippines, while younger age groups (18–34) were overrepresented, the observed population change trends remained reliable, as this demographic typically exhibits higher mobility [30]. Moreover, the usage of these social media data in government reports [22] during the COVID-19 pandemic further proved the value of the results derived from them.

Moreover, changes in Facebook usage throughout the study period may have influenced the results. People confined to their homes during lockdowns led to greater use of social media [22]. Although we eliminated changes from the collected data by normalising the population numbers, the possible uneven changes across different areas over time might skew the results. However, there is no evidence that Facebook usage trends varied spatially. Similarly, a study on mobile location data from SafeGraph in the United States showed that the relative sampling rate across geographic levels appeared relatively stable from 2020 to 2022 [67].

Despite inherent uncertainties in the data and the limitations of the analyses outlined above, the findings and insights from our study, based on a novel location dataset, provide a new cross-national perspective on population change patterns on various urban density in response to the shock of COVID-19. Our research helps identify countries that have experienced or are more likely to experience population redistribution out of highly urbanised areas, and highlights the importance of adaptable rural-urban planning and policy frameworks that account for shifting population dynamics to address future challenges to societal and environmental sustainability.

Methods

Facebook population data at tile level

Facebook population data were aggregated spatially to Bing tile levels [68] by Meta across 8-hour periods during the COVID-19 pandemic. The spatial tile level and time period varied for different countries (see Supplementary Table 5), adapting to ensure computation updates within an 8-hour window and compliance with privacy standards. In general, our samples ranged from tile level 12 (approximately 9.8 km at the equator) to tile level 16 (approximately 600 m at the equator). Time periods also varied by country and began in March, April, or May of 2020 and extended to the 21stor 22nd of May 2022. For each 8-hour period (00:00–07:59, 08:00–15:59, 16:00–23:59 Coordinated Universal Time), the number of individual devices in each tile was collected. These devices correspond with a Facebook app user who has consented to share their mobile device location history with Meta. Locations are estimated using signals like Wi-Fi and mobile networks, GPS and sensor information where available. If a user appeared in different tiles during one time window, their location was assigned to the tile where they appeared most frequently. These data come with an associated baseline count, which is defined as the average number of users for at least 90 days before the start of data collection in each country [21]. Additionally, Meta applied privacy protection techniques, excluding any population or baseline lower than ten people for a specific time and date to ensure that the locations of individuals or small groups cannot be identified [21]. To avoid bias caused by excluded values in rural areas, we applied a two-step imputation procedure, as described in ref. [20], to estimate missing data for specific dates. First, the baseline count for a tile with missing data was estimated either from valid observations on other dates or, when unavailable, from a linear regression between Facebook baseline counts and WorldPop 2019 population data [69] within each country. Second, missing value was reconstructed using the imputed baseline together with its corresponding percent change from baseline reported by Facebook for that date. Further imputation details are provided in ref. [20] and, for convenience, in Supplementary Note 1.

We then analysed the population changes during the night-time window on workdays in each country to explore residential redistribution, considering that people are likely to be at home during that time. The workdays are not identical across the globe; specific workdays for each country can be found in Supplementary Table 5. We excluded the half-working day, such as Friday in the United Arab Emirates, to more accurately capture their normal living location. We used the aggregated weekly averages of daily populations on workdays to capture the main residence and reduce the effect of occasional overnight/late night trips on our results. Additionally, the procedure to eliminate the seasonal variation based on weekly observations (see the details below) and the use of robust linear regression for trend estimation (see below) also helped reduce the impact of variations during holiday periods.

Moreover, the total population counts collected showed an overall trend and daily fluctuations due to limitations in internet access and active user availability [21,22]. To address this, we normalised the counts to eliminate changes caused by data collection [20], assuming that the representativeness of Facebook data for each tile remained constant throughout the period. Specifically, we adjusted the counts for each tile on a given date by first calculating each tile's share of the total daily population across all tiles, and then scaled these proportions by the median of the daily total population observed throughout the study period [20]. Thus, these adjusted numbers represent the population redistribution [70], control for changes in Facebook usage, and are used to infer distribution patterns across different urban density areas.

Study areas

A total of 35 countries were selected based on the following criteria related to data availability and quality: 1) the availability of Facebook population data at the tile level from Meta [21]; 2) Facebook data covering more than two years to allow for the detection and removal of seasonal variations; 3) data with a spatial resolution at Bing tile level 12 or higher (approximately <=9.8 km at the equator)[68], as too coarse spatial details cannot provide effective information; 4) an estimated high penetration of Facebook usage (over 40% of the total population) [62], which will likely reduce potential bias in using Facebook data to infer population-level mobility. The 40% penetration threshold was selected to optimise the trade-off between high platform penetration and a sufficient sample size for cross-national analysis. At this level, only two countries were excluded compared to the 30% threshold (from 37 to 35), whereas increasing it to 50% would have resulted in a much larger loss of eight countries, reducing the sample to 27 (Supplementary Fig. 17). The final sample of 35 countries contains 15.3% of the global population [1], including 23 high-income countries and 12 middle-income countries. Notably, these criterial resulted in the exclusion of low-income countries, which generally have low smartphone adoption rates [71] and very limited Facebook usage [62]. Several major countries such as the United States, China and India were also excluded due to data unavailability or low Facebook penetration. Furthermore, we conducted a sensitivity analysis using the 27 countries that met a stricter 50% penetration criterion to confirm the robustness of our predictor effects (Supplementary Fig. 18).

Urban density and urban-rural definitions

We chose to use percentage cover of built-up areas at each country's spatial tiles to characterise their degrees of urbanisation. The Esri 2020 Land Cover dataset was selected due to its higher accuracy in built-up areas (95.8% user's accuracy and 83.7% producer's accuracy) compared to other land use and land cover datasets of 2020 [72]. This global map, derived from European Space Agency (ESA) Sentinel-2 imagery at 10m resolution, provides 9 classes of land cover. The class "built-up area" includes human made structures, major road and rail networks, and large homogenous impervious surfaces [72].

In this study, urban areas are defined as areas with more than 25% built-up areas [37], based on a commonly used definition from the perspective of physical urban land [37,38]. It is important to note that this classification reflects the degree of physical urban density for each tile, without considering their contiguity (neighbouring tiles).

Response phases segmentation and population change calculation

To divide the study period into distinct of pandemic response, we identified abrupt changes in weekly urban population proportion data (2020–2022) for each country using the Breaks For Additive Seasonal and Trend (BFAST) algorithm [73]. This data-driven segmentation was conducted to account for the impacts of COVID-19 restrictions, recognising that identical restrictions might have different effects across pandemic waves and countries [34,35,74]. BFAST was implemented using the "BFAST" package in R.

The BFAST algorithm first applied Seasonal-Trend decomposition using Loess (STL) [75] to eliminate the seasonal variation for our weekly Facebook population data [20]. STL is widely used in trend analysis

because it is not sensitive to outliers, applicable to various seasonal data types, and computationally efficient [76,77]. Detailed STL procedures are described in Cleveland et al., (1990).

BFAST then tested for any abrupt changes in the deseasoned data using the Moving SUM (MOSUM) approach [78]. The sensitivity of breakpoint detection was controlled by the minimum interval setting. We selected this setting based on a sensitivity analysis that tested intervals ranging from 10% to 50% of the total study period for each country (Supplementary Fig. 13). An interval of 40% (approximately 44 weeks) yielded the most stable and consistent results across countries (Supplementary Fig. 14) and was therefore used in this study. This interval also effectively captured dominant shifts while filtering out minor fluctuations. When a significant change was detected ($P < 0.05$), the breakpoint was estimated by minimising the Bayesian Information Criterion (BIC) [79]. This involved an iterative procedure that minimised the residual sum of squares to estimate the optimal break positions and their 95% confidence intervals. In most countries in our analysis, BFAST identified one significant breakpoint, which we used to define two analytical phases: Phase 1 (early response) preceding the break; and Phase 2 (later response) following it.

Finally, changes were quantified using slopes and *P* values from robust linear regression fitted to the pre- and post-breakpoint segments. The robust linear regression, performed by "MASS" package in R, offers greater robustness to outliers, helping to mitigate the impact of unexpected events like holidays [80].

To segment phases and analyse changes in urban-rural population redistributions, we calculated the weekly population proportion (*Pro*) in urban areas,

$$Pro = \sum_{i=1}^{N} \left(S_{n,i} \times X_i\right) \Big/ \sum_{i=1}^{N} \left(S_{n,i}\right) \quad (1)$$

where X_i = 1 if the urban density of tile *i* is exceeding 25%, and X_i = 0 otherwise. *N* is the total number of tiles for this country, and $S_{n,i}$ is the Facebook population counts for tile *i*. Changes in *Pro* (Indicator 1) summarised country-level changes in urban-rural population distributions.

To assess finer-scale changes in population density along the urban density gradient, we analysed tile-level population counts for tiles with adequate data coverage, that is, those with at least two complete periods required to identify seasonal components. We applied robust linear regression at each tile to estimate changes in population density within the phases defined by the breakpoint of its respective country. These were used to explore finer-scale dynamics along the urban density gradient. Spearman correlation coefficients between these changes and the corresponding urban density values (Indicator 2) were computed to summarise country-level patterns along the urban density gradient.

Statistical analyses of country-level differences

To explore the relationship between two indicators of country-level redistribution patterns, we fitted Bayesian linear models using the "brms" package in R [81], with default non/weakly informative priors. The response variable was the Spearman correlation between population change and urban density (Indicator 2), and the predictor was the change in urban population proportions (Indicator 1). Their standard errors (SEs) were estimated separately from the "vcmeta" package [82] and robust linear

regression. Models for both response phases were run using four chains, each with 2000 iterations and 1000 warm-up iterations.

We also assessed the extent to which Indicator 1 and 2 were associated with country-level socioeconomic characteristics across the two response phases, using four additional Bayesian multivariate linear models [83]. Each indicator served as the response variable in separate models, with their SEs as measurement errors. Based on previous research, we selected eight potential explanatory variables spanning socioeconomic conditions, industrial structure, culture, governance, and COVID-19 interventions [36] (see Supplementary Table 7 for data sources). We included the Human Development Index (HDI) [46], as most studies on urban-to-rural redistribution have primarily focused on countries in the Global North, which are typically characterised by higher levels of social and economic development. To capture aspects of inequality not reflected in the HDI [84], we added income inequality [85], a major component of urban–rural gap that can drive migration [86]. Industrial structure was measured using the share of industry value and the share of agriculture, forestry, and fishing value, to capture the degree of economic transformation, as shifts from agriculture- to industry- or services-led economies often increase urban pull factors [50,87,88]. We also included unemployment to account for economically motivated migration [48,89]; individualism [90], as evidence links higher residential mobility to societies that prioritise individual autonomy over collective identity [91,92]; and government effectiveness, to capture the quality of public services and policy implementation that determine regional liveability and appeal to potential migrants [52,93]. Finally, to capture the impact of pandemic policy, we used the COVID-19 stringency index [36], which reflects the severity of government-imposed restrictions likely to influence residential decisions. To account for multicollinearity of these variables, we calculated pair-wise Pearson correlations and the variance inflation factor (VIF) in linear regressions. We excluded variables with a correlation coefficient higher than 0.7 (individualism, government effectiveness and the share of agriculture, forestry value; Supplementary Fig. 9), with all retained variables had a VIF below 2.5. For completeness, we report a sensitivity analysis in the Supplementary Fig. 10 where each excluded variable was substituted into the model in place of its highly correlated counterpart. All predictors were standardised prior to modelling.

These models were run with four Markov chains, each with 2,000 iterations and 1,000 warm-up iterations, using default priors. Convergence on all four chains was achieved for each model (rhat = 1.00 for all coefficient estimates). Given our limited sample size and to avoid overfitting, we selected the final models based on the lowest leave-one-out cross-validation information criterion (LOOIC; calculated using R package "loo" [94]) after assessing all possible predictor combinations. As a sensitivity analysis, we presented competing models with similarly low LOOIC scores in Supplementary Fig. 8 to confirm that the effects of key predictors were robust across different model specifications.

Data availability

The Facebook population data (tile level) for this study were obtained through Meta's AI for Good program. They are not publicly available due to licensing agreements. Information on requesting access to this data can be found at https://dataforgood.facebook.com/. All other data used in this paper are publicly available, with sources listed in the text. These include the Esri 2020 Land Cover dataset (https://livingatlas.arcgis.com/landcover/), the Human Development Index (https://hdr.undp.org/data-center/human-development-index#/indicies/HDI), income inequality data from the Standardized World

Income Inequality Database v.9.8 (https://doi.org/10.7910/DVN/LM4OWF), government effectiveness, unemployment, share of industry, share of agriculture, forestry, and fishing data from the World Bank (https://data.worldbank.org/indicator), Geert Hofstede's Individualism versus Collectivism scores (https://geerthofstede.com/culture-geert-hofstede-gert-jan-hofstede/6d-model-of-national-culture/), and COVID-19 stringency index from the Oxford Covid-19 Government Response Tracker (https://www.bsg.ox.ac.uk/research/covid-19-government-response-tracker). Country and administrative boundaries were sourced from the Global Administrative Areas spatial database (https://gadm.org/data.html).

Acknowledgments

This work was supported by the ESRC South Coast Doctoral Training Partnership (grant number ES/P000673/1), as part of the first author's doctoral research, and the National Institute for Health (MIDAS Mobility R01AI160780) and the Horizon Europe (UKRI grant number 10041831). SL and AJT are supported by funding from the Bill & Melinda Gates Foundation (OPP1134076, INV-024911), the National Institutes of Health (R01AI160780), the Horizon Europe program (MOOD 874850) and the U.S. National Science Foundation (DMS-2327797). The authors would like to also acknowledge the AI for Good program at Meta for sharing data and thank Dr Tim O'Riordan, Dr Eimear Cleary, Dr Theo Chan, and Dr Fatumah Atuhaire for Facebook population data collection. We thank Yuxuan Guo, Dr Nick Dorward, Dr Rebecca Collins and Dr Sarchil Qader for discussions and suggestions that improved the manuscript. The icons used in Figure 1 were designed by Freepik, Nikita Golubev, mnauliady, kerismaker, Karyative, Prosymbols Premium, DinosoftLabs, juicy_fish, Vectors Market, Dewi Sari, and Sudowoodo from www.flaticon.com.

Author information

Authors and Affiliations
School of Geography and Environmental Science, University of Southampton, Southampton SO17 1BJ, United Kingdom
Qianwen Duan & Felix Eigenbrod

WorldPop, School of Geography and Environmental Science, University of Southampton, Southampton SO17 1BJ, United Kingdom
Shengjie Lai, Andrew J. Tatem & Jessica Steele

Dipartimento di Scienze della Terra "Ardito Desio", Università degli Studi di Milano, Via Mangiagalli 34, 20133 Milan, Italy
Alessandro Sorichetta

Contributions
QD, SL, AS and FE contributed to conceptualisation. QD and FE designed the research. QD, SL and AJT contributed to Facebook data curation. QD conducted formal analysis, visualisation and wrote the

manuscript. FE, SL and JS helped to improve the methodology. All authors commented on and revised drafts of the manuscript.

Corresponding author
Correspondence to Qianwen Duan

Ethics declarations

The authors declare no competing interests.

References

1. World Bank. World Bank Open Data. (2022).
2. Wahba Tadros, S. N. *et al. Demographic Trends and Urbanization*. http://documents.worldbank.org/curated/en/260581617988607640/Demographic-Trends-and-Urbanization (2021).
3. Halfacree, K. To revitalise counterurbanisation research? Recognising an international and fuller picture. *Population, Space and Place* **14**, 479–495 (2008).
4. Rowe, F., Bell, M., Bernard, A., Charles-Edwards, E. & Ueffing, P. Impact of internal migration on population redistribution in Europe: Urbanisation, counterurbanisation or spatial equilibrium? *CPoS* **44**, (2019).
5. Niva, V. *et al.* World's human migration patterns in 2000–2019 unveiled by high-resolution data. *Nat Hum Behav* **7**, 2023–2037 (2023).
6. Sutradhar, U., Spearing, L. & Derrible, S. Depopulation and associated challenges for US cities by 2100. *Nat Cities* **1**, 51–61 (2024).
7. Gamlen, A. Migration isn't increasing, border restrictions don't reduce crossings — and other home truths. *Nature* **623**, 683–684 (2023).
8. Wolff, M. & Mykhnenko, V. COVID-19 as a game-changer? The impact of the pandemic on urban trajectories. *Cities* **134**, 104162 (2023).

9. Stawarz, N., Rosenbaum-Feldbrügge, M., Sander, N., Sulak, H. & Knobloch, V. The impact of the COVID-19 pandemic on internal migration in Germany: A descriptive analysis. *Population, Space and Place* **28**, e2566 (2022).
10. Ilham, M. A., Fonzone, A., Fountas, G. & Mora, L. To move or not to move: A review of residential relocation trends after COVID-19. *Cities* **151**, 105078 (2024).
11. Güneralp, B., Reba, M., Hales, B. U., Wentz, E. A. & Seto, K. C. Trends in urban land expansion, density, and land transitions from 1970 to 2010: a global synthesis. *Environ. Res. Lett.* **15**, 044015 (2020).
12. Cheng, L., Yang, M., De Vos, J. & Witlox, F. Examining geographical accessibility to multi-tier hospital care services for the elderly: A focus on spatial equity. *Journal of Transport & Health* **19**, 100926 (2020).
13. Herrero-Jáuregui, C. & Concepción, E. D. Effects of counter-urbanization on Mediterranean rural landscapes. *Landsc Ecol* **38**, 3695–3711 (2023).
14. Huang, S. *et al.* Widespread global exacerbation of extreme drought induced by urbanization. *Nat Cities* **1**, 597–609 (2024).
15. Jimenez, Y. G. *et al.* Counterurbanization: A neglected pathway of forest transition. *Ambio* **51**, 823–835 (2022).
16. Faust, K. M., Abraham, D. M. & DeLaurentis, D. Coupled Human and Water Infrastructure Systems Sector Interdependencies: Framework Evaluating the Impact of Cities Experiencing Urban Decline. *Journal of Water Resources Planning and Management* **143**, 04017043 (2017).
17. Leyk, S. *et al.* The spatial allocation of population: a review of large-scale gridded population data products and their fitness for use. *Earth System Science Data* **11**, 1385–1409 (2019).
18. Lai, S. *et al.* Assessing the Effect of Global Travel and Contact Restrictions on Mitigating the COVID-19 Pandemic. *Engineering (Beijing)* **7**, 914–923 (2021).

19. Cot, C., Cacciapaglia, G. & Sannino, F. Mining Google and Apple mobility data: temporal anatomy for COVID-19 social distancing. *Sci Rep* **11**, 4150 (2021).

20. Duan, Q. *et al.* Identifying counter-urbanisation using Facebook's user count data. *Habitat International* **150**, 103113 (2024).

21. Maas, P. Facebook Disaster Maps: Aggregate Insights for Crisis Response & Recovery. in *Proceedings of the 25th ACM SIGKDD International Conference on Knowledge Discovery & Data Mining* 3173–3173 (ACM, Anchorage AK USA, 2019). doi:10.1145/3292500.3340412.

22. Shepherd, H. E. R., Atherden, F. S., Chan, H. M. T., Loveridge, A. & Tatem, A. J. Domestic and international mobility trends in the United Kingdom during the COVID-19 pandemic: an analysis of facebook data. *International Journal of Health Geographics* **20**, 46 (2021).

23. Jia, S., Kim, S. H., Nghiem, S. V., Doherty, P. & Kafatos, M. C. Patterns of population displacement during mega-fires in California detected using Facebook Disaster Maps. *Environ. Res. Lett.* **15**, 074029 (2020).

24. Rashid, M. M., Tirtha, S. D., Eluru, N. & Hasan, S. Understanding hurricane evacuation behavior from Facebook data. *International Journal of Disaster Risk Reduction* **116**, 105147 (2025).

25. Jamal, T. B. & Hasan, S. Understanding the loss in community resilience due to hurricanes using Facebook Data. *International Journal of Disaster Risk Reduction* **97**, 104036 (2023).

26. Gibbs, H. *et al.* Detecting behavioural changes in human movement to inform the spatial scale of interventions against COVID-19. *PLOS Computational Biology* **17**, e1009162 (2021).

27. Rowe, F., Calafiore, A., Arribas-Bel, D., Samardzhiev, K. & Fleischmann, M. Urban exodus? Understanding human mobility in Britain during the COVID-19 pandemic using Meta-Facebook data. *Population, Space and Place* **29**, e2637 (2023).

28. Silva, L., Bezzo, F. B., Manfredini, F., Giavarini, V. & Di Rosa, C. Away from the cities? A medium-to-long-term investigation of how the COVID-19 pandemic has changed population spatial patterns in Italy. *European Urban and Regional Studies* **32**, 147–165 (2025).
29. Beria, P. & Lunkar, V. Presence and mobility of the population during the first wave of Covid-19 outbreak and lockdown in Italy. *Sustainable Cities and Society* **65**, 102616 (2021).
30. Dujardin, S., Vibar, A. A. B., Paulus, R., Kienberger, S. & Linard, C. Dynamic Social Vulnerability Mapping Using Facebook Data. *Population, Space and Place* **31**, e70022 (2025).
31. Cabrera, C., Rowe, F., González-Leonardo, M., Nasuto, A. & Neville, R. Long-term disparities in the recovery of urban mobility after COVID-19 in Latin America. Preprint at https://doi.org/10.48550/arXiv.2504.15871 (2025).
32. Zhou, Y. *et al.* Satellite mapping of urban built-up heights reveals extreme infrastructure gaps and inequalities in the Global South. *Proceedings of the National Academy of Sciences* **119**, e2214813119 (2022).
33. Xu, G. *et al.* Underlying rules of evolutionary urban systems in Africa. *Nat Cities* **2**, 327–335 (2025).
34. Ge, Y. *et al.* Untangling the changing impact of non-pharmaceutical interventions and vaccination on European COVID-19 trajectories. *Nat Commun* **13**, 3106 (2022).
35. Kim, S., Jang, K. & Yeo, J. Non-linear impacts of COVID-19 pandemic on human mobility: Lessons from its variations across three pandemic waves. *Sustainable Cities and Society* **97**, 104769 (2023).
36. Hale, T. *et al.* A global panel database of pandemic policies (Oxford COVID-19 Government Response Tracker). *Nat Hum Behav* **5**, 529–538 (2021).
37. Schneider, A., Friedl, M. A. & Potere, D. Mapping global urban areas using MODIS 500-m data: New methods and datasets based on 'urban ecoregions'. *Remote Sensing of Environment* **114**, 1733–1746 (2010).

38. Zhang, X. *et al.* A large but transient carbon sink from urbanization and rural depopulation in China. *Nat Sustain* **5**, 321–328 (2022).

39. Ghosh, T. S., Shanahan, F. & O'Toole, P. W. Toward an improved definition of a healthy microbiome for healthy aging. *Nat Aging* **2**, 1054–1069 (2022).

40. Dutilleul, P., Clifford, P., Richardson, S. & Hemon, D. Modifying the t Test for Assessing the Correlation Between Two Spatial Processes. *Biometrics* **49**, 305–314 (1993).

41. Arel-Bundock, V., Enevoldsen, N. & Yetman, C. countrycode: An R package to convert country names and country codes. *Journal of Open Source Software* **3**, 848 (2018).

42. Gkartzios, M. & Halfacree, K. Editorial. Counterurbanisation, again: Rural mobilities, representations, power and policies. *Habitat International* **140**, 102906 (2023).

43. Halfacree, K. Counterurbanisation in post-covid-19 times. Signifier of resurgent interest in rural space across the global North? *Journal of Rural Studies* **110**, 103378 (2024).

44. Lucas, R. E., Jr. Life earnings and rural-urban migration. *Journal of political economy* **112**, S29–S59 (2004).

45. Dilley, L., Gkartzios, M. & Odagiri, T. Developing counterurbanisation: Making sense of rural mobility and governance in Japan. *Habitat International* **125**, 102595 (2022).

46. United Nations Development Programme. *Human Development Report 2019: Beyond Income, beyond Averages, beyond Today: Inequalities in Human Development in the 21st Century*. https://hdr.undp.org/system/files/documents/hdr2019.pdf (2019).

47. Rees, P. *et al.* The Impact of Internal Migration on Population Redistribution: an International Comparison. *Population, Space and Place* **23**, e2036 (2017).

48. Gkartzios, M. 'Leaving Athens': Narratives of counterurbanisation in times of crisis. *Journal of Rural Studies* **32**, 158–167 (2013).

49. Anastasiou, E. & Duquenne, M.-N. Determinants and Spatial Patterns of Counterurbanization in Times of Crisis: Evidence from Greece. *Population Review* **59**, (2020).
50. Sun, Y., Jiao, L., Guo, Y. & Xu, Z. Recognizing urban shrinkage and growth patterns from a global perspective. *Applied Geography* **166**, 103247 (2024).
51. Does financial development increase energy consumption? The role of industrialization and urbanization in Tunisia. *Energy Policy* **40**, 473–479 (2012).
52. Pang, Y., Zhang, W. & Jiang, H. A socio-spatial exploration of rural livability satisfaction in megacity Beijing, China. *Ecological Indicators* **158**, 111368 (2024).
53. Tripathi, S. How does urbanization affect the human development index? A cross-country analysis. *Asia-Pac J Reg Sci* **5**, 1053–1080 (2021).
54. Mahendra, A. *et al.* Seven transformations for more equitable and sustainable cities. (2021).
55. Lima, M. F. & Eischeid, M. R. Shrinking cities: rethinking landscape in depopulating urban contexts. *Landscape Research* **42**, 691–698 (2017).
56. Zasada, I. *et al.* International retirement migration in the Alicante region, Spain: process, spatial pattern and environmental impacts. *Journal of Environmental Planning and Management* **53**, 125–141 (2010).
57. Yu, L., Wang, Y. & Li, M. The emergence of counter-urbanisation in China: Can it be a pathway for rural revitalisation? *Habitat International* **144**, 102998 (2024).
58. Rasambainarivo, F. *et al.* Prioritizing COVID-19 vaccination efforts and dose allocation within Madagascar. *BMC Public Health* **22**, 724 (2022).
59. Petherick, A. *et al.* A worldwide assessment of changes in adherence to COVID-19 protective behaviours and hypothesized pandemic fatigue. *Nat Hum Behav* **5**, 1145–1160 (2021).
60. Shi, Y. *et al.* Lockdown policy in pandemics: Enforcement, adherence, and effectiveness in the case of COVID-19. *Infectious Disease Modelling* **10**, 493–504 (2025).

61. Nikiforiadis, A. *et al.* Exploring mobility pattern changes between before, during and after COVID-19 lockdown periods for young adults. *Cities* **125**, 103662 (2022).

62. World Population Review. Facebook Users by Country 2023. https://worldpopulationreview.com/country-rankings/facebook-users-by-country (2023).

63. Schiavina, M., Freire, S., Carioli, A. & MacManus, K. GHS-POP R2023A - GHS population grid multitemporal (1975-2030). European Commission, Joint Research Centre (JRC) https://doi.org/10.2905/2FF68A52-5B5B-4A22-8F40-C41DA8332CFE (2023).

64. Roskams, M. Population and household estimates, England and Wales: Census 2021. *Office for National Statistics* (2022).

65. Office for National Statistics (ONS). *Origin-Destination Data, England and Wales: Census 2021*. https://www.ons.gov.uk/peoplepopulationandcommunity/populationandmigration/populationestimates/bulletins/origindestinationdataenglandandwales/census2021#origin-destination-migration-data (2023).

66. Ribeiro, F. N., Benevenuto, F. & Zagheni, E. How Biased is the Population of Facebook Users? Comparing the Demographics of Facebook Users with Census Data to Generate Correction Factors. in *Proceedings of the 12th ACM Conference on Web Science* 325–334 (Association for Computing Machinery, New York, NY, USA, 2020). doi:10.1145/3394231.3397923.

67. Li, Z., Ning, H., Jing, F. & Lessani, M. N. Understanding the bias of mobile location data across spatial scales and over time: A comprehensive analysis of SafeGraph data in the United States. *PLOS ONE* **19**, e0294430 (2024).

68. Bing Maps Tile System - Bing Maps. https://learn.microsoft.com/en-us/bingmaps/articles/bing-maps-tile-system (2022).

69. WorldPop. Global High Resolution Population Denominators Project - Funded by The Bill and Melinda Gates Foundation (OPP1134076). (2020) doi:10.5258/SOTON/WP00660.

70. Reia, S. M., Rao, P. S. C., Barthelemy, M. & Ukkusuri, S. V. Spatial structure of city population growth. *Nat Commun* **13**, 5931 (2022).

71. Milusheva, S., Björkegren, D. & Viotti, L. Can We Trust Smartphone Mobility Estimates in Low-Income Countries. *World Bank Blogs* https://blogs.worldbank.org/en/opendata/can-we-trust-smartphone-mobility-estimates-low-income-countries (2021).

72. Karra, K. *et al.* Global land use / land cover with Sentinel 2 and deep learning. in *2021 IEEE International Geoscience and Remote Sensing Symposium IGARSS* 4704–4707 (2021). doi:10.1109/IGARSS47720.2021.9553499.

73. Verbesselt, J., Hyndman, R., Newnham, G. & Culvenor, D. Detecting trend and seasonal changes in satellite image time series. *Remote Sensing of Environment* **114**, 106–115 (2010).

74. McKenzie, G. & Adams, B. A country comparison of place-based activity response to COVID-19 policies. *Applied Geography* **125**, 102363 (2020).

75. Cleveland, R. B., Cleveland, W. S., McRae, J. E. & Terpenning, I. STL: A seasonal-trend decomposition. *Journal of Official Statistics* **6**, 3–73 (1990).

76. Boulton, C. A., Lenton, T. M. & Boers, N. Pronounced loss of Amazon rainforest resilience since the early 2000s. *Nat. Clim. Chang.* **12**, 271–278 (2022).

77. Woods, D. *et al.* Exploring methods for mapping seasonal population changes using mobile phone data. *Humanit Soc Sci Commun* **9**, 1–17 (2022).

78. Zeileis, A. A unified approach to structural change tests based on ML scores, F statistics, and OLS residuals. *Econometric Reviews* **24**, 445–466 (2005).

79. Bai, J. & Perron, P. Computation and analysis of multiple structural change models. *Journal of applied econometrics* **18**, 1–22 (2003).

80. Yu, C. & Yao, W. Robust linear regression: A review and comparison. *Communications in Statistics - Simulation and Computation* **46**, 6261–6282 (2017).

81. Bürkner, P.-C. brms: An R Package for Bayesian Multilevel Models Using Stan. *Journal of Statistical Software* **80**, 1–28 (2017).

82. Bonett, D. G. vcmeta: Varying Coefficient Meta-Analysis. 1.4.0 https://doi.org/10.32614/CRAN.package.vcmeta (2021).

83. Grünwald, J., Hanzelka, J., Voříšek, P. & Reif, J. Long-term population trends of 48 urban bird species correspond between urban and rural areas. *iScience* **27**, 109717 (2024).

84. Hicks, D. A. The inequality-adjusted human development index: A constructive proposal. *World Development* **25**, 1283–1298 (1997).

85. Solt, F. Measuring Income Inequality Across Countries and Over Time: The Standardized World Income Inequality Database. *Social Science Quarterly* **101**, 1183–1199 (2020).

86. Wan, G., Zhang, X. & Zhao, M. Urbanization can help reduce income inequality. *npj Urban Sustain* **2**, 1 (2022).

87. Xu, H. & Jiao, M. City size, industrial structure and urbanization quality—A case study of the Yangtze River Delta urban agglomeration in China. *Land Use Policy* **111**, 105735 (2021).

88. Borck, R., Pflüger, M. & Wrede, M. A simple theory of industry location and residence choice. *Journal of economic geography* **10**, 913–940 (2010).

89. Mitchell, C. J. A. Making sense of counterurbanization. *Journal of Rural Studies* **20**, 15–34 (2004).

90. Hofstede, G. Country comparison. *Hofstede insights* (2018).

91. Tang, S. S., Zhou, J. & Liu, Y. Emerging in-migration of urban young adults engaging in rural tourism in China. *Population, Space and Place* **30**, e2791 (2024).

92. Oishi, S. The Psychology of Residential Mobility: Implications for the Self, Social Relationships, and Well-Being. *Perspect Psychol Sci* **5**, 5–21 (2010).

93. Chen, Z. & Paudel, K. P. Economic openness, government efficiency, and urbanization. *Review of Development Economics* **25**, 1351–1372 (2021).

94. Vehtari, A. *et al.* loo: Efficient leave-one-out cross-validation and WAIC for Bayesian models. *(No Title)* (2015).